

## ORIGINAL ARTICLE

# ARF1 controls proliferation of breast cancer cells by regulating the retinoblastoma protein

P-L Boulay<sup>1</sup>, S Schlienger<sup>1</sup>, S Lewis-Saravalli<sup>1</sup>, N Vitale<sup>2</sup>, G Ferbeyre<sup>3</sup> and A Claing<sup>1,3</sup>

<sup>1</sup>Department of Pharmacology, Faculty of Medicine, University of Montreal, Montréal, Québec, Canada; <sup>2</sup>Institut des Neurosciences Cellulaires et Intégratives Unité Propre de Recherche-3212 Centre National de la Recherche Scientifique Université de Strasbourg, Strasbourg, France and <sup>3</sup>Department of Biochemistry, Faculty of Medicine, University of Montreal, Montréal, Québec, Canada

The ADP-ribosylation factors (ARFs) 1 and 6 are small GTP-binding proteins, highly expressed and activated in several breast cancer cell lines and are associated with enhanced migration and invasiveness. In this study, we report that ARF1 has a critical role in cell proliferation. Depletion of this GTPase or expression of a dominant negative form, which both resulted in diminished ARF1 activity, led to sustained cell-growth arrest. This cellular response was associated with the induction of senescent markers in highly invasive breast cancer cells as well as in control mammary epithelial cells by a mechanism regulating retinoblastoma protein (pRB) function. When examining the role of ARF1, we found that this GTPase was highly activated in normal proliferative conditions, and that a limited amount could be found in the nucleus, associated with the chromatin of MDA-MB-231 cells. However, when cells were arrested in the G<sub>0</sub>/G<sub>1</sub> phase or transfected with a dominant negative form of ARF1, the total level of activated ARF1 was markedly reduced and the GTPase significantly enriched in the chromatin. Using biochemical approaches, we demonstrated that the GDP-bound form of ARF1 directly interacted with pRB, but not other members of this family of proteins. In addition, depletion of ARF1 or expression of ARF1<sup>T31N</sup> resulted in the constitutive association of pRB and E2F1, thereby stabilizing the interaction of E2F1 as well as pRB at endogenous sites of target gene promoters, preventing expression of E2F target genes, such as cyclin D1, Mcm6 and E2F1, important for cell-cycle progression. These novel findings provide direct physiological and molecular evidence for the role of ARF1 in controlling cell proliferation, dependent on its ability to regulate pRB/E2F1 activity and gene expression for enhanced proliferation and breast cancer progression.

*Oncogene* (2011) 30, 3846–3861; doi:10.1038/onc.2011.100; published online 11 April 2011

**Keywords:** ADP-ribosylation factor; breast cancer; cell cycle; proliferation; retinoblastoma protein

## Introduction

Cell division is a physiological process that occurs in almost all tissues and under many circumstances. Under normal conditions, the balance between proliferation and programmed cell death is maintained by tightly regulating both processes to ensure the integrity of organs and tissues. Activation or upregulation of oncogenes disrupts these orderly processes by disrupting the program regulating cell-cycle entry and death. The conversion of normal cells into tumor cells involves changes in the activity of a number of different genes and proteins. One of the best characterized oncogenes is the small GTP-binding protein Ras (Der *et al.*, 1982; Parada *et al.*, 1982). Its uncontrolled activation and/or upregulation promote the transformation of a pre-malignant to a malignant phenotype. Ectopic expression of H-Ras induces senescence in normal fibroblast (Serrano *et al.*, 1997). Several other GTPases have been linked to cancer progression. For example, members of the Rho family of proteins were found to regulate adhesion and motility (Azab *et al.*, 2009; Larrea *et al.*, 2009; Myhre and Blobel, 2009; Wu *et al.*, 2009). We and others recently reported that ADP-ribosylation factors (ARF), another family of small GTP-binding proteins, are highly expressed in cancer cells and regulate migration, invasion as well as proliferation (Hashimoto *et al.*, 2004; D'Souza-Schorey and Chavrier, 2006; Boulay *et al.*, 2008). These proteins are different from the alternate reading frame tumor-suppressor protein, also known as p14<sup>ARF</sup>, initially identified as an alternative transcript of the *INK4a/ARF* tumor-suppressor locus (Duro *et al.*, 1995).

Like all GTPases, ARF proteins cycle between an inactive GDP-bound and an active GTP-bound state through the dynamic interaction of guanine-nucleotide exchange factors and GTPase-activating proteins, respectively. ARF1 and ARF6 are the most studied isoforms. ARF1 is mainly found in the Golgi apparatus and acts to promote carrier vesicle biogenesis by nucleating the assembly of coat protein complexes at sites of vesicle formation (Stearns *et al.*, 1990). Several reports have suggested that ARF1 can also localize to the plasma membrane transmitting signals from transmembrane proteins (Galas *et al.*, 1997; Mitchell *et al.*, 2003; Cohen *et al.*, 2007; Boulay *et al.*, 2008).

Correspondence: Professor A Claing, Department of Pharmacology, Faculty of Medicine, University of Montreal, PO Box 6128, Downtown station, Montreal, Québec, Canada H3C 3J7.

E-mail: audrey.claing@umontreal.ca

Received 2 June 2010; revised 11 February 2011; accepted 3 March 2011; published online 11 April 2011

In invasive breast cancer cells, stimulation of the epidermal growth factor receptor leads to the activation of ARF1, the PI3K pathway, and ultimately cell migration and proliferation (Boulay *et al.*, 2008). Alternatively, ARF6, the isoform classically associated with the plasma membrane, is activated by this receptor to stimulate activation of the mitogen-activated protein kinase (MAPK) pathway (Hashimoto *et al.*, 2004; D'Souza-Schorey and Chavrier, 2006; Boulay *et al.*, 2008).

Activation of the PI3K/Akt pathway by growth factors is associated with cell survival and growth (that is, an increase in cell mass), as well as proliferation through multiple downstream targets impinging on cell-cycle regulation (Manning and Cantley, 2007). Namely, Akt potently drive cell proliferation by regulating the cyclin-dependent kinase inhibitor p27<sup>kip1</sup> (Liang *et al.*, 2002; Narita *et al.*, 2002; Yakes *et al.*, 2002; Motti *et al.*, 2005) and the ubiquitin ligase Mdm2 (Zhou *et al.*, 2001). In addition, Akt inhibits CHK1 activity, a cell-cycle checkpoint (Tonic *et al.*, 2010), as well as many other effects. Furthermore, activation of the PI3K–Akt–mTOR–p70<sup>S6K</sup> signaling axis controls the function of the retinoblastoma protein (pRB), a central regulator of cell-cycle progression. At the molecular level, pRB is recognized as a pivotal regulator of G<sub>1</sub> checkpoint, thereby inhibiting S phase entry and cell-cycle progression (Weinberg, 1995). RB function is controlled by upstream cyclin-dependent kinases that are activated during the G<sub>0</sub>/G<sub>1</sub> transition phase. When in a hypophosphorylated state, pRB inhibits proliferation by repressing the activity of E2F transcription factors, limiting expression of cell-cycle regulatory genes, such as cyclin A, cyclin D1, cyclin E, Mcm5 and Mcm6 (Nevins *et al.*, 1991; Ohtani *et al.*, 1995, 1999; Watanabe *et al.*, 1998), essentials for progression from G<sub>1</sub> into S phase (Weinberg, 1995). Hyperphosphorylation of pRB (ppRB) results in the dissociation of E2Fs, allowing transactivation of E2F targets and transition through G<sub>1</sub>/S phases of the cell cycle. It is now believed that pRB has many additional roles, such as control of cellular differentiation, regulation of apoptotic cell death, maintenance of permanent cell-cycle arrest, and preservation of chromosomal stability (Burkhart and Sage, 2008).

In benign tumors, the process of senescence, which is characterized by an irreversible growth-arrest program, occurs following oncogene activation or telomere shortening. Cellular senescence therefore acts to restrict tumor progression. Recently, we have shown that benign prostate tumors are senescent and have low E2F gene expression (Vernier *et al.*, 2011). In advanced cancers, this defense mechanism is bypassed by mutations in tumor suppressor genes (Courtois-Cox *et al.*, 2008). Senescence is regulated by a complex signaling network and characterized by a persistent activation of the DNA damage signaling pathway (Mallette and Ferbeyre, 2007), chromatin remodeling through the formation of senescence-associated heterochromatin foci (SAHF) (Narita *et al.*, 2003), and an increase of lysosomal  $\beta$ -galactosidase ( $\beta$ -gal) (Dimri and Campisi, 1994). Although SAHF help to maintain E2F targets in

a repressed state, other mechanisms contribute to the overall inhibition of E2Fs in senescence. The activation state of pRB can be altered by disrupting signaling through the cyclin D/p16<sup>INK4a</sup>/pRB pathway (Takano *et al.*, 1999). Cellular senescence takes several days to establish, and in oncogene-expressing cells, usually follows an initial cell proliferation phase (Ferbeyre *et al.*, 2002). Once initiated, this program cannot be reversed by the cell (Ferbeyre *et al.*, 2002; Sun *et al.*, 2007).

In this study, we have investigated the molecular mechanisms by which the small GTP-binding protein ARF1 regulates proliferation of an invasive breast cancer cell line, MDA-MB-231 (negative for estrogen receptor, progesterone receptor and Her2/Neu receptor). Triple negative tumors constitute 12–24% of breast cancers and show aggressive clinical behavior, such as lung and bone metastasis formation. These tumors are not responsive to available therapies (Yagata *et al.*, 2011). The identification of novel pharmacological targets is therefore urgent. Here, we show that by lowering active levels of ARF1, by either using RNA interference or overexpression of a dominant negative mutant, proliferation of MDA-MB-231 was markedly reduced by mechanisms involving senescence. This permanent cell growth arrest was associated with the inhibition of pRB hyperphosphorylation, dissociation of pRB/E2F1 protein complex, constitutive association of E2F1 and pRB with target gene promoters, and expression of E2F responsive genes. In addition, we show that ARF1 can directly interact with pRB and translocate to the nucleus during G<sub>0</sub>/G<sub>1</sub> phase. The understanding of the molecular mechanism by which ARF1 controls tumor cell proliferation, especially senescence induction, is important for the development of future anti-breast cancer therapies.

## Results

### *ARF1 regulates breast cancer cell proliferation*

To define the role of ARF1 in breast cancer cell proliferation, we first examined the effect of depleting this GTPase in the MDA-MB-231 cell line. As reported previously, endogenous ARF1 expression was reduced by 90%, 3 days following transfection of our small interfering RNA (siRNA) (Figure 1a) (Boulay *et al.*, 2008). As illustrated in Figure 1b, cells transfected with a control siRNA gradually proliferated over a 12-day period. During the first 6 days following transfection, depletion of ARF1 did not significantly impair the proliferation rate of MDA-MB-231 cells. However, ARF1 knockdown markedly reduced the ability of the cells to proliferate from day 7–12, the later time point we examined. The effect of depleting ARF1 was prevented by overexpressing an siRNA-insensitive ARF1 construct (ARF1 mutant), demonstrating specificity. We also examined proliferation of human breast epithelial cells, MCF10A, an immortalized and non-transformed cell line, harboring no mutation in the *Ras* and *HER2*

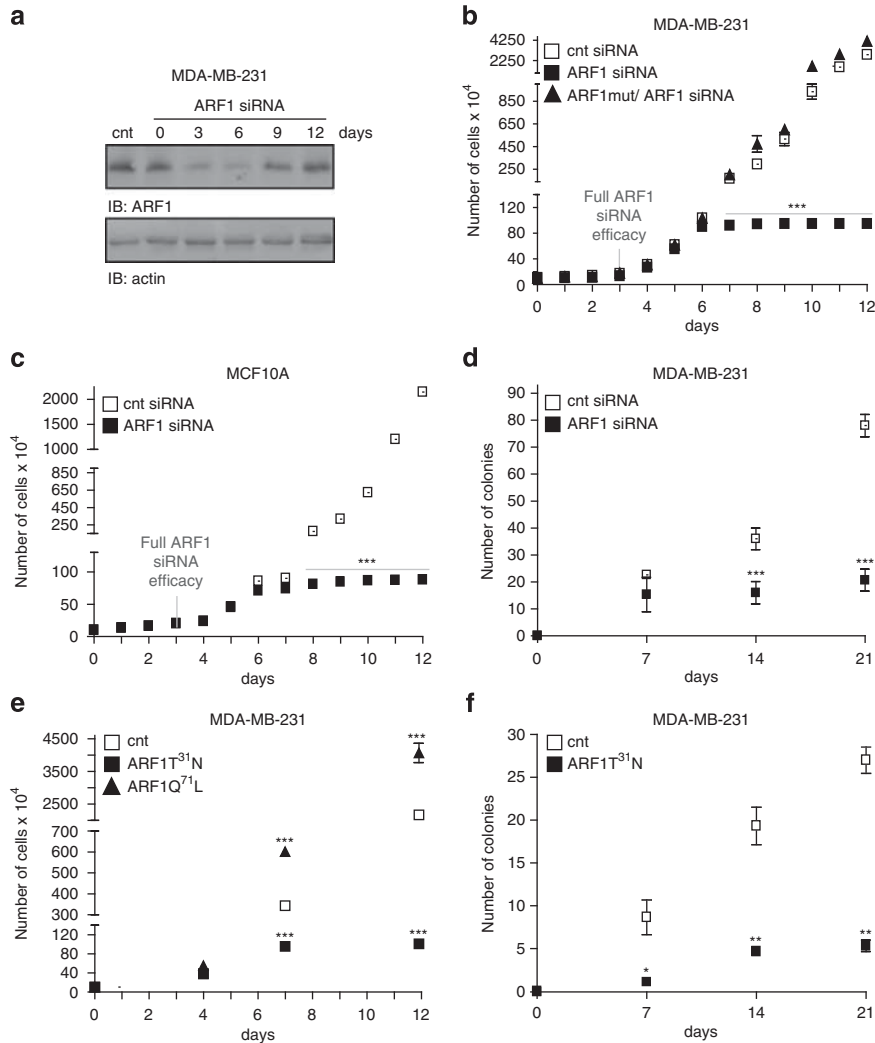


**Figure 1** ARF1 regulates cell proliferation. **(a)** MDA-MB-231 cells were transfected with a scrambled (cnt) or ARF1 siRNA. Endogenous expression of ARF1 and actin was examined by western blotting, 0, 3, 6, 9 and 12 day(s) after siRNA transfection. These results are representative of three independent experiments. **(b)** MDA-MB-231 cells were transfected with a scrambled (cnt), ARF1 siRNA or ARF1 siRNA together with ARF1 mutant. Cells were reseeded into a 10-cm dish and left to grow for 12 days. Cell proliferation was represented as the number of cells for each transfection condition, as indicated. These results are the mean  $\pm$  s.e.m. of three independent experiments. \*\*\* $P < 0.001$  are values compared with the paired control siRNA transfection condition. **(c)** MCF10A cells were transfected with a scrambled (cnt) or ARF1 siRNA, and proliferation was assessed as in **(a)**. Results are the mean  $\pm$  s.e.m. of three independent experiments. \*\*\* $P < 0.001$  are values compared with the paired control siRNA transfection condition. **(d)** MDA-MB-231 cells were transfected with either a scrambled (cnt) or ARF1 siRNA and were plated onto soft agar. Fresh media was added and cells were left for 21 days. Results are the mean  $\pm$  s.e.m. of three independent experiments. \*\*\* $P < 0.001$  are values compared with the paired control siRNA transfection condition. **(e)** MDA-MB-231 cells were transfected with an empty vector (cnt), ARF1<sup>Q71L</sup> or ARF1<sup>T31N</sup>. Cell proliferation was assessed as in **(c)**. Results are the mean  $\pm$  s.e.m. of three independent experiments. \*\*\* $P < 0.001$  are values compared with the paired control siRNA transfection condition. **(f)** MDA-MB-231 cells were transfected with an empty vector or ARF1<sup>T31N</sup> and allowed to grow onto soft agar as in **(d)**. Results are the mean  $\pm$  s.e.m. of three independent experiments. \* $P < 0.05$ , \*\* $P < 0.01$  are values compared with the paired empty vector control condition.

genes (Soule *et al.*, 1990). As illustrated in Figure 1c, depletion of ARF1 significantly blocked the proliferation of MCF10A cells, an effect observed 7 days post transfection. In these cells, ARF1 siRNA reduced by 81% the endogenous levels of protein, 3 days after the transfection (Supplementary Figure 1). We next examined the ability of the MDA-MB-231 cells to form colonies on soft agar to assess anchorage-independent cell proliferation. ARF1-depleted cells were significantly impaired in their ability to form colonies, over a 21-day

period, compared with control transfections (Figure 1d). Finally, we examined the effect of overexpressing a constitutively active (ARF1<sup>Q71L</sup>) and a dominant negative (ARF1<sup>T31N</sup>) form of this GTPase in MDA-MB-231 cells. As illustrated in Figure 1e, ARF1<sup>Q71L</sup> expression led to enhance cell proliferation, whereas ARF1<sup>T31N</sup> expression was inhibitory. We next examined the effect of this later ARF1 mutant in colony formation on soft-agar media. ARF1<sup>T31N</sup> inhibited the ability of MDA-MB-231 cells to form spots of colonies

over a 21-day period compared with the control condition (empty vector) (Figure 1f).

To determine whether this growth arrest we observed in ARF1-depleted or -inactivated cells was associated with the induction of senescence, we next examined more closely cell entry into this program known to prevent unlimited cell proliferation.

*Depletion of ARF1 promotes cellular senescence*

First, we performed a senescence-associated- $\beta$ -gal (SA- $\beta$ -gal) activity assay to measure levels of this lysosomal enzyme found to be more active in senescent cells. As illustrated in Figure 2a, no staining was observed in the control condition (non-transfected MDA-MB-231 cells), demonstrating that in normal conditions, these cells are not senescent, but proliferate normally. The tumor suppressor p16<sup>INK4a</sup>, a cyclin-dependent kinase inhibitor

known to induce G<sub>1</sub> arrest, was reported to be deleted in MDA-MB-231 cells (Supplementary Figure 2A) (Hui *et al.*, 2000). As expected, its overexpression increased the number of SA- $\beta$ -gal/senescent-positive MDA-MB-231 cells (Figure 2a). Inhibition of ARF1 expression resulted in senescence of MDA-MB-231 cells; a process observed 4 days after transfection of the siRNA, but maximal after 7 days. This effect was completely prevented by overexpressing the oncoviral protein E7, which promoted the degradation of pRB through the ubiquitin-proteasome pathway (Boyer *et al.*, 1996). Depletion of ARF1 was also effective in inducing  $\beta$ -gal activity in SKBR3 cells, a cell line known to express high levels of p16<sup>INK4a</sup> (Supplementary Figure 2B) (Hui *et al.*, 2000). We also assessed the effect of overexpressing the dominant negative form of ARF1. Expression of ARF1<sup>T31N</sup> increased the number of

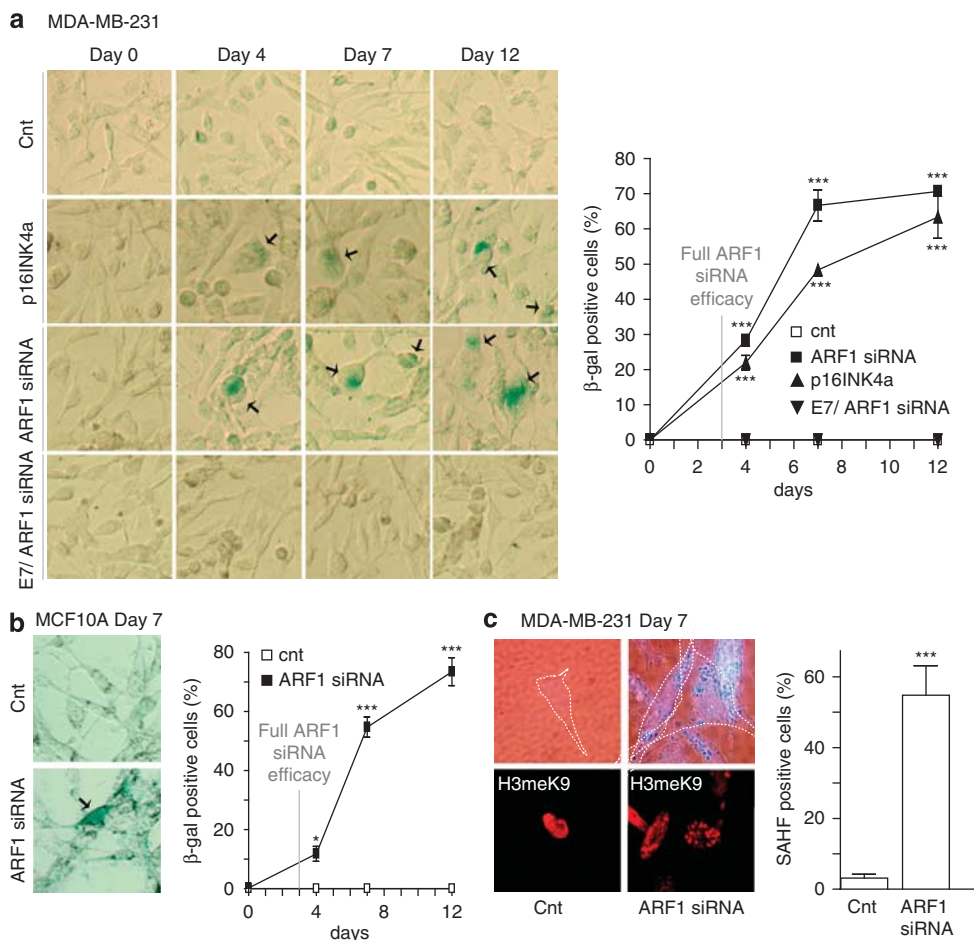


**Figure 2** ARF1 depletion leads to cellular senescence. (a) MDA-MB-231 cells were transfected or not with an ARF1 siRNA, or infected with p16<sup>INK4a</sup>. In some conditions, ARF1-depleted cells were infected with E7. Cells were fixed and assessed for  $\beta$ -gal activity detection. Images represent pictures from five different fields taken after 0, 4, 7 and 12 day(s) post transfection or post infection.  $\beta$ -gal-positive blue cells are marked by a black arrow. Quantifications represent the number of  $\beta$ -gal-positive cells. Results are the mean  $\pm$  s.e.m. of seven independent experiments. \*\*\* $P$ <0.001 are values compared with the paired non-transfected condition. (b) MCF10A cells were transfected or not with an ARF1 siRNA. After the indicated times, cells were fixed and assessed for  $\beta$ -gal activity as in (a). Results are the mean  $\pm$  s.e.m. of three independent experiments. \* $P$ <0.05, \*\*\* $P$ <0.001 are values compared with the paired control siRNA transfection condition. (c) MDA-MB-231 cells were transfected with a scrambled (cnt) or ARF1 siRNA, fixed and stained with X-gal (contrast phase image) and anti-H3meK9 antibody (immunofluorescence image) 7 days post transfection. Quantification represents the percentage of cells that exhibited the SAHF phenotype. Images represent pictures from five different fields taken. These results are representative of six independent experiments. \*\*\* $P$ <0.001 are values compared with the cnt siRNA transfection condition.

senescent MDA-MB-231 cells (Supplementary Figure 3A). We next performed SA- $\beta$ -gal activity assays in MCF10A cells. As illustrated in Figure 2b, no activity was detected in control siRNA conditions. In contrast, ARF1 depletion increased the number of SA- $\beta$ -gal-positive cells. Representative pictures from SA- $\beta$ -gal staining, 7 days post transfection, are shown.

Senescent cells have flattened shape and exhibit heterochromatin foci formation called SAHF. These heterochromatic regions are characterized by an enrichment of histone H3 methylated on lysine-9 (H3meK9) (Narita *et al.*, 2003). We examined SAHF to confirm that depletion of ARF1 can engage breast cancer cells senescence. As illustrated in Figure 2c, control cells presented a normal cell shape (phase contrast picture) and a diffuse nuclear pattern of H3meK9 staining, where no chromatin condensation was observed. In contrast, cells transfected with ARF1 siRNAs harbored a flat shape (phase contrast picture) and displayed foci of heterochromatic regions enriched in H3meK9. Quantification of positive SAHF cells revealed that under ARF1 depletion, 54% of the cells harbored this phenotype. Finally, we examined the number of SAHF-positive cells when ARF1T<sup>31N</sup> was expressed. We observed that in these conditions, 53% of the cells were positive (Supplementary Figure 3B). Taken together, our data show that the number of senescent cells, assessed by SA- $\beta$ -gal activity, correlates with the quantification of SAHF-positive cells.

The rescue of the senescence phenotype by E7 and the presence of SAHF suggested a role for pRB in the senescence response induced by ARF1 depletion or expression of an inactive form. To define the molecular mechanism by which endogenously expressed ARF1 controls cellular proliferation, we next examined the association of pRB with the transcription factor E2F1, known to regulate cell-cycle progression.

#### *The association of pRB and E2F1 is regulated by ARF1*

The main function of the pRB protein is to bind and inhibit transcription factors of the E2F family. Upon cells entry into S phase, pRB becomes hyperphosphorylated and allows E2F to dissociate and initiate transcription of target genes that facilitate the G<sub>1</sub>/S transition and S phase. We first examined the role of ARF1 in controlling pRB hyperphosphorylation, and its subsequent association with E2F1. When cells were in the presence of serum-containing media, pRB was highly phosphorylated on Ser 795 (ppRB). Depletion of ARF1 markedly inhibited this effect (Figure 3a). In addition, when cells overexpressed a constitutively activated or a dominant negative form of ARF1, hyperphosphorylation of pRB was enhanced or diminished, respectively, when compared with the control condition (empty vector) (Figure 3a). Third, when cells were arrested in the G<sub>0</sub>/G<sub>1</sub> phase (no serum), pRB and E2F1 remained associated, thereby preventing cell-cycle progression (Figure 3b). In contrast, when cells were in the presence of serum (cnt), pRB was dissociated from E2F1. Four days after transfection of ARF1 siRNA, pRB was already found constitutively in complex with

E2F1 (Figure 3b). This effect was prevented when an ARF1 construct, insensitive to the siRNA, was expressed. To define whether the association of pRB to E2F1 was dependent upon the presence of the GTPase or its ability to become activated, we expressed the ARF1 mutants mimicking the GDP- and GTP-bound form. Expression of ARF1T<sup>31N</sup> resulted in the association of pRB and E2F1, whereas the active form of the GTPase prevented the interaction (Figure 3b), suggesting that activation of the GTPase promotes dissociation of the pRB/E2F1 complex. Similar observations were obtained 7 days post transfection (data not shown).

In these experiments, we systematically observed a small but significant decrease of total pRB expression when ARF1 siRNA was transfected (Supplementary Figure 4A), whereas levels of p107 and p130 remained unaffected (data not shown). We therefore examined whether decreased levels of total pRB were the result of altered gene expression or increased degradation by performing quantitative reverse transcriptase-PCR. The levels of pRB mRNA transcripts were found to be similar in control and ARF1 siRNA-transfected cells, 4 days after transfection (Supplementary Figure 4B). Depletion of ARF1 led to increased ubiquitination of pRB, a process maximal 4 days after transfection (Supplementary Figure 4C).

To further understand the role of ARF1 in regulating cell-cycle progression, we examined the expression profile of E2F1 responsive genes, cyclin D1, Mcm6 and E2F1, known to respectively regulate cyclin-dependent kinases, initiation of genome replication, and gene transcription. Depletion of ARF1 significantly reduced the expression of these genes both at the protein (Figure 3c) and mRNA levels (Figure 3d). Notably, these effects were only observed after 6 and 7 days of siRNA transfection, the time point at which a maximal number of cells are senescent.

Altogether, these data suggested to us that the level of activated ARF1 might change during cell-cycle progression to modulate the association of pRB and E2F1, and subsequent cell-cycle gene transcription.

#### *Activation and cellular distribution of ARF1 during cell-cycle progression*

To better understand the role of endogenously expressed ARF1 in MDA-MB-231 cells, we examined the activation profile of this GTPase through the cell cycle. We first used GST-pulldown assays to assess ARF1-GTP levels during G<sub>0</sub>/G<sub>1</sub>, G<sub>1</sub>/S and M phases. MDA-MB-231 cells were maintained in fresh media containing serum (cnt), synchronized in the G<sub>0</sub>/G<sub>1</sub> phase using serum-starving media or treated with cell-cycle inhibitors hydroxyurea and vincristine to synchronize cells in G<sub>1</sub>/S and M phase, respectively. As described in Figure 4a, ARF1-GTP levels were found to be higher in control conditions where cells can proliferate normally. In contrast, activated ARF1 levels were significantly lower when cells were arrested in the G<sub>0</sub>/G<sub>1</sub> phase, but gradually increased during the G<sub>1</sub>/S and M phases. We next examined the cellular localization of the GTPase. We overexpressed ARF1-Flag and performed

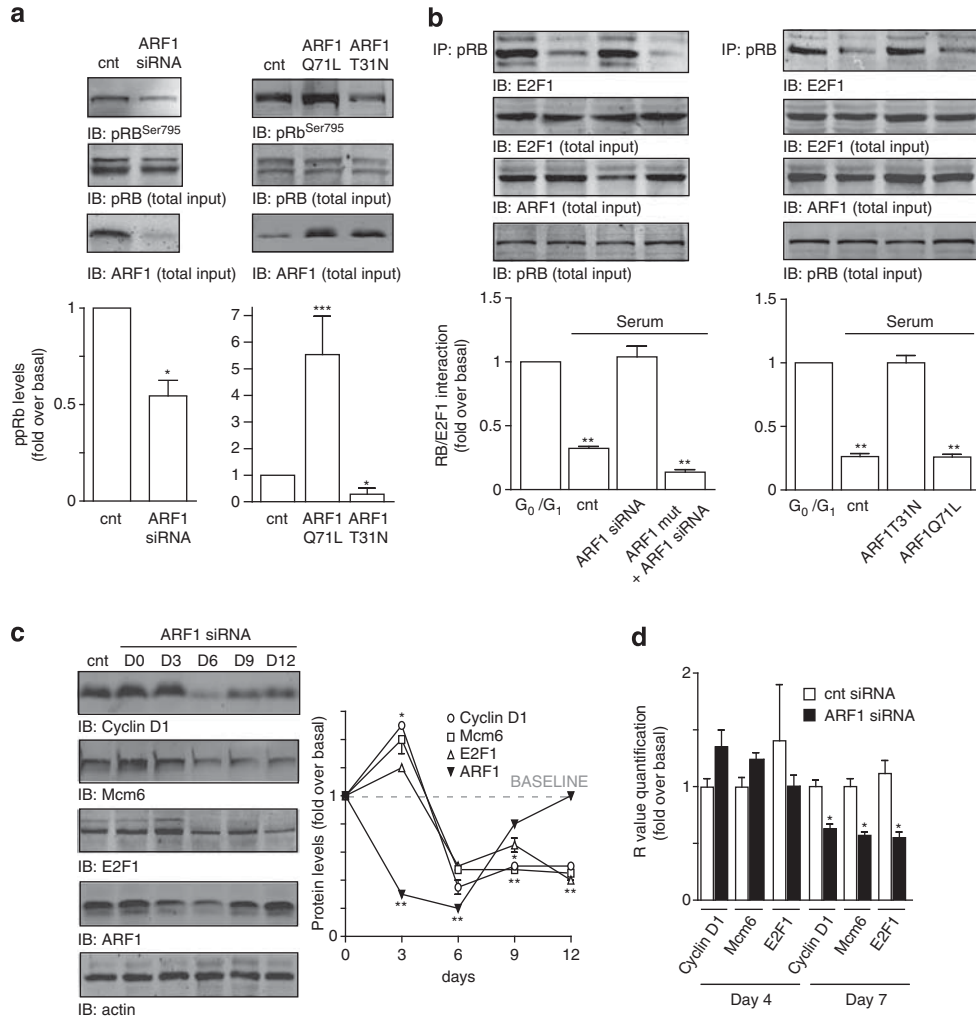


**Figure 3** The association of pRB and E2F1 is regulated by ARF1. **(a)** MDA-MB-231 cells were transfected with a control siRNA, ARF1 siRNA, empty vector, ARF1<sup>Q71L</sup> or ARF1<sup>T31N</sup>. Cells were then harvested and levels of pRB hyperphosphorylated on Ser 795 assessed by western blotting. Quantifications are the mean  $\pm$  s.e.m. of four independent experiments. \* $P$ <0.05, \*\*\* $P$ <0.001 are values compared with the cnt condition. **(b)** MDA-MB-231 cells were transfected with ARF1 siRNA, ARF1 siRNA and ARF1 mutant, ARF1<sup>T31N</sup> or ARF1<sup>Q71L</sup>. Endogenous pRB was immunoprecipitated and interacting E2F1 was detected using western blot analysis. Quantifications are the mean  $\pm$  s.e.m. of four independent experiments. \*\* $P$ <0.01 are values compared with non-transfected cells treated under serum-starved condition. **(c)** Cells were transfected with a scrambled (cnt) or ARF1 siRNA. Endogenous expression of cyclin D1, Mcm6, E2F1, ARF1 and actin were examined by western blotting 0, 3, 6, 9 and 12 days after siRNA transfection. The control condition was assessed 3 days post transfection. Quantifications are the mean  $\pm$  s.e.m. of three independent experiments. \* $P$ <0.05, \*\* $P$ <0.01 are values compared with the scrambled (cnt). **(d)** MDA-MB-231 cells were transfected with a scrambled (cnt) or ARF1 siRNA. mRNA levels of cyclin D1, Mcm6 and E2F1 were assessed by quantitative real-time PCR after 4 and 7 days post transfection. Data are presented as relative mRNA levels, and are the mean  $\pm$  s.e.m. of three independent experiments. \* $P$ <0.05, when compared with the cnt condition.

cell fractionation assays to assess ARF1 distribution in the soluble, nuclear and chromatin fractions. First, levels of ARF1-Flag were found similar in the soluble fraction of cells proliferating normally (cnt) or arrested in the different phases of the cell cycle (Figure 4b). However, when cells were arrested in the G<sub>0</sub>/G<sub>1</sub> or M phase, amounts of ARF1-Flag were found increased in the nuclear fraction, in contrast to GM130, a Golgi marker present in large amounts in the membrane fraction, but also in the cytosolic fraction (Figure 4b and Supplementary Figure 5A). We next extracted chromatin from the nucleus and observed that ARF1-Flag levels were increased when cells were arrested in G<sub>0</sub>/G<sub>1</sub>,

as well as the M phase (Supplementary Figure 5B). Using a specific ARF1 antibody, we examined the distribution of endogenously expressed ARF1. Similarly to what we observed when ARF1 was overexpressed, the amount of endogenous ARF1 in the chromatin was increased during the G<sub>0</sub>/G<sub>1</sub>, but not during M phase (Figure 4c). Lastly, we examined the distribution of ARF1 using confocal microscopy. In normal conditions and at the confocal plane we examined, much of the endogenous ARF1 protein was found in the Golgi (single green spot), next to the nucleus (Figure 4d). However, when cells were synchronized in the G<sub>0</sub>/G<sub>1</sub> phase (no serum), ARF1 was localized to the nucleus.

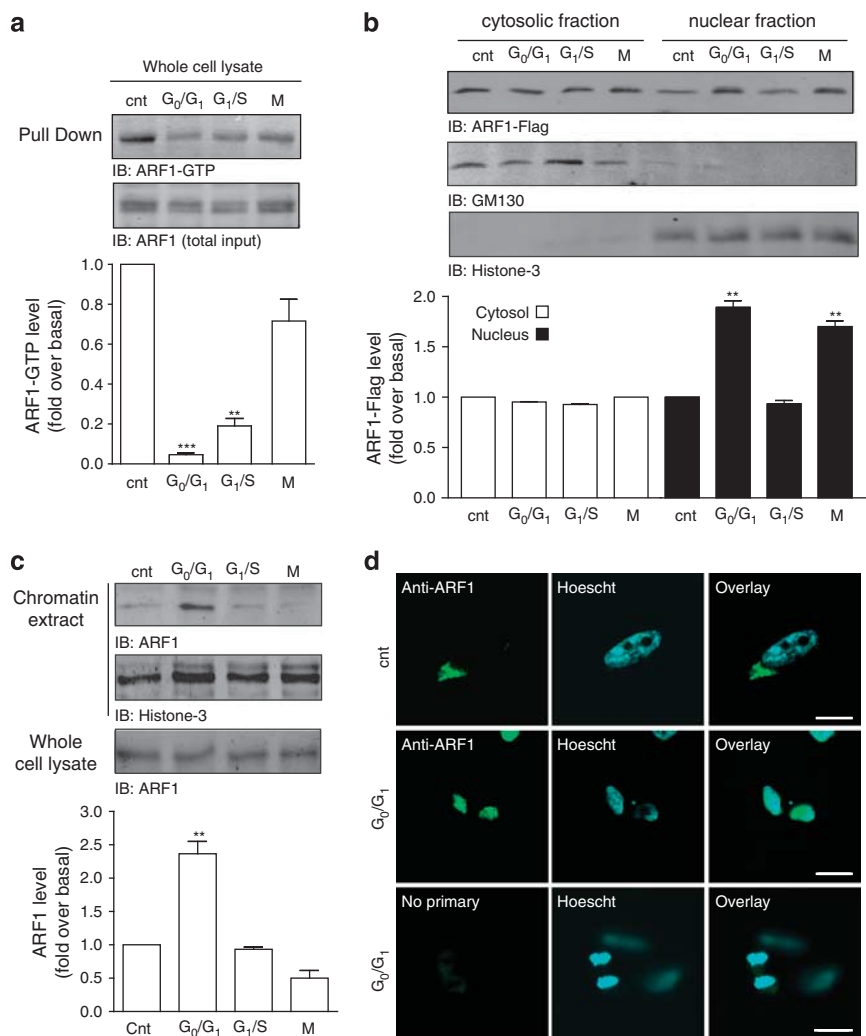


**Figure 4** Redistribution of ARF1 in the nucleus in non-proliferative conditions. **(a)** MDA-MB-231 cells were arrested in the different phases of the cell cycle or left in normal serum conditions. ARF1-GTP levels were detected by western blotting using a specific anti-ARF1 antibody. Quantifications are the mean  $\pm$  s.e.m. of three independent experiments.  $**P < 0.01$ ,  $***P < 0.001$  are values compared with the cnt-untreated condition for each cell fraction. **(b)** Cells were transfected with ARF1-Flag and treated as in **(a)**. Cytosolic and nuclear cellular fractions were prepared and the presence of ARF1 examined. Quantifications are the mean  $\pm$  s.e.m. of three independent experiments.  $**P < 0.01$  are values compared with the control untreated cells. **(c)** Cells were left in normal serum conditions or arrested in different phases of the cell cycle. Chromatin was isolated, and endogenously expressed ARF1 as well as Histone-3 were detected in each condition by western blotting. Quantifications are the mean  $\pm$  s.e.m. of three independent experiments.  $**P < 0.01$  are values compared with the cnt-untreated cells. **(d)** Cells were treated or not with serum for 16 h, fixed, stained for ARF1, and counter stained with Hoescht. Scale bar represents 10  $\mu$ m. These images are representative of 20 cells observed in three independent experiments.

Altogether, these results suggest that the activity of ARF1 is modulated during the different phases of the cell cycle, although protein levels remain constant. In addition, our data suggest that depending on its activation state, this GTPase can be relocalized to different cellular compartments.

We next examined the possibility that ARF1 might interact with pRB. In these experiments, pRB or other members of the family were immunoprecipitated and amounts of interacting ARF1 detected by western blot analysis. In control conditions, when cells were allowed to proliferate normally, endogenously expressed ARF1 did not interact with pRB, p107 or p130 (Figure 5a). However, arrest in the G<sub>0</sub>/G<sub>1</sub> phase led to the formation of a complex including pRB and ARF1. In these

experiments, p107 and p130 did not interact with the GTPase. To determine whether the activation state of ARF1 may modulate its ability to interact with pRB in chromatin extracts, we overexpressed the dominant negative and constitutively active mutants of ARF1. When cells were arrested in the G<sub>0</sub>/G<sub>1</sub> phase, endogenously expressed ARF1 was also found in the chromatin extract, in complex with pRB. Similar results were observed when ARF1<sup>T31N</sup> was expressed (Figure 5b). In contrast, ARF1<sup>Q71L</sup> did not relocalize to the chromatin and interact with pRB. When cells were allowed to proliferate normally (cnt), endogenously expressed ARF1 did not interact with pRB, possibly because low levels of ARF1 were present within the chromatin in these conditions. However, the inactive mutant

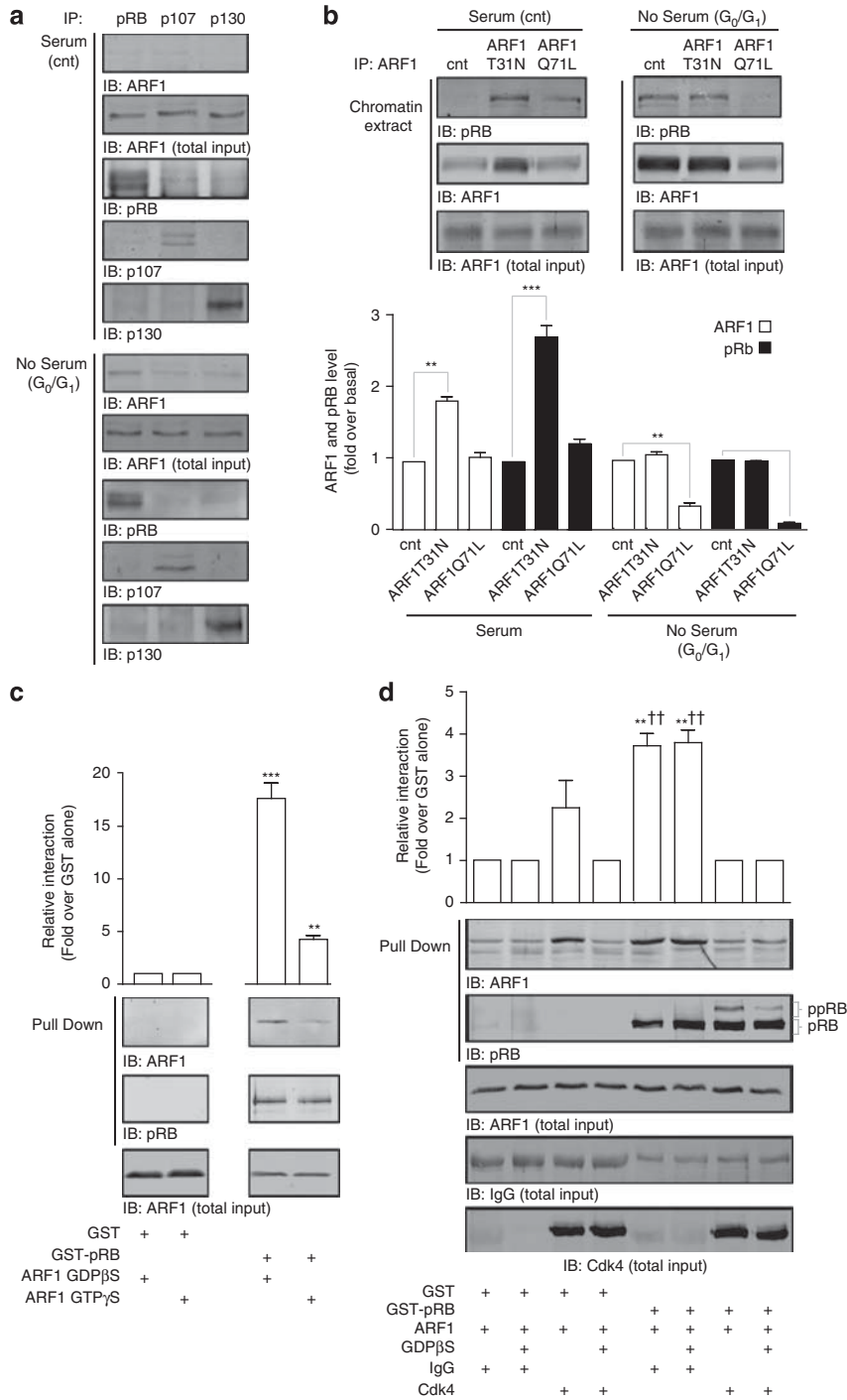


**Figure 5** ARF1 directly interacts with pRB. (a) MDA-MB-231 cells were left in normal serum conditions or arrested in the G<sub>0</sub>/G<sub>1</sub> phase. Endogenously expressed pRB, p107 or p130 were immunoprecipitated and interacting ARF1 was detected by western blotting. This experiment is representative of two others. (b) Cells were transfected with empty vector (cnt), ARF1T<sup>31N</sup> or ARF1Q<sup>71L</sup> and treated or not with serum for 16 h. ARF1 (endogenous or expressed clones) was immunoprecipitated from the chromatin extract and interacting pRB was detected by western blotting. Quantifications are the mean ± s.e.m. of three independent experiments. \*\**P*<0.01, \*\*\**P*<0.001 are values compared with the paired empty vector transfection condition. (c) GST-pRB was incubated with ARF1 (loaded with GDPβS or GTPγS) and the interaction was detected by western blotting. Quantifications are the mean ± s.e.m. of four independent experiments. \*\**P*<0.01 and \*\*\**P*<0.001 are values compared with the paired control GST. (d) GST-pRB was incubated with immunoprecipitated Cdk4 or IgG and then mixed with ARF1 (loaded or not with GDPβS). The interaction was detected by western blot analysis. Quantifications are the mean ± s.e.m. of three independent experiments. \*\**P*<0.001 are values compared with the GST, ARF1 and IgG condition. ††*P*<0.01 are values compared with the GST-pRB, ARF1 and IgG condition.

(ARF1T<sup>31N</sup>), but not the constitutively active form of ARF1 (ARF1Q<sup>71L</sup>), was found in the chromatin and interacted with pRB (Figure 5b). Using confocal microscopy, ARF1T<sup>31N</sup> was found to be present in the nucleus of proliferating MDA-MB-231 cells, in contrast to ARF1 (Supplementary Figure 6A). In COS-7 cells, which expressed large T antigen known to inhibit the growth-regulatory function of pRB (Gluzman, 1981; Chellappan *et al.*, 1992; Miller *et al.*, 2007), the ARF1 mutant was not found in the nucleus but perinuclearly (Supplementary Figure 6B). To further determine whether the endogenous expression of pRB could regulate the enrichment of endogenous ARF1 or ARF1T<sup>31N</sup> in chromatin, we next overexpressed E7 to specifically decrease pRB level. When MDA-MB-231 cells were synchronized in the G<sub>0</sub>/G<sub>1</sub> phase (no serum) or allowed to proliferate (serum), overexpression of E7 prevented the enrichment of ARF1 and ARF1T<sup>31N</sup> in chromatin (Supplementary Figure 6C). We next examined whether ARF1 and pRB could directly interact using purified proteins. As illustrated in Figure 5c,

GST-pRB interacted preferentially with the GDP-bound form of the GTPase. Because the phosphorylation status of pRB impacts its ability to interact with binding partners, we investigated whether the interaction between ARF1 and pRB could be modulated by the phosphorylation state of pRB. As illustrated in Figure 5d, phosphorylation of GST-pRB by Cdk4, immunoprecipitated from MDA-MB-231 cells, abolished its ability to interact with ARF1. Altogether, these data demonstrate that in some conditions, ARF1 can interact with pRB.

*ARF1 regulates the stability of the association of pRB/E2F1 to its target gene promoters*

We next investigated whether ARF1 could regulate the association of E2F1 and pRB to promoters of *cyclin D1* and *Mcm6* genes, using chromatin immunoprecipitation (ChIP) assays. PCR analysis revealed that in control growing cells, a fraction of E2F1, but not pRB, interacts with cyclin D1 and Mcm6 promoters (Figure 6a). Depletion of ARF1 resulted in the stabilization of the interaction between E2F1 and its target gene promoters.

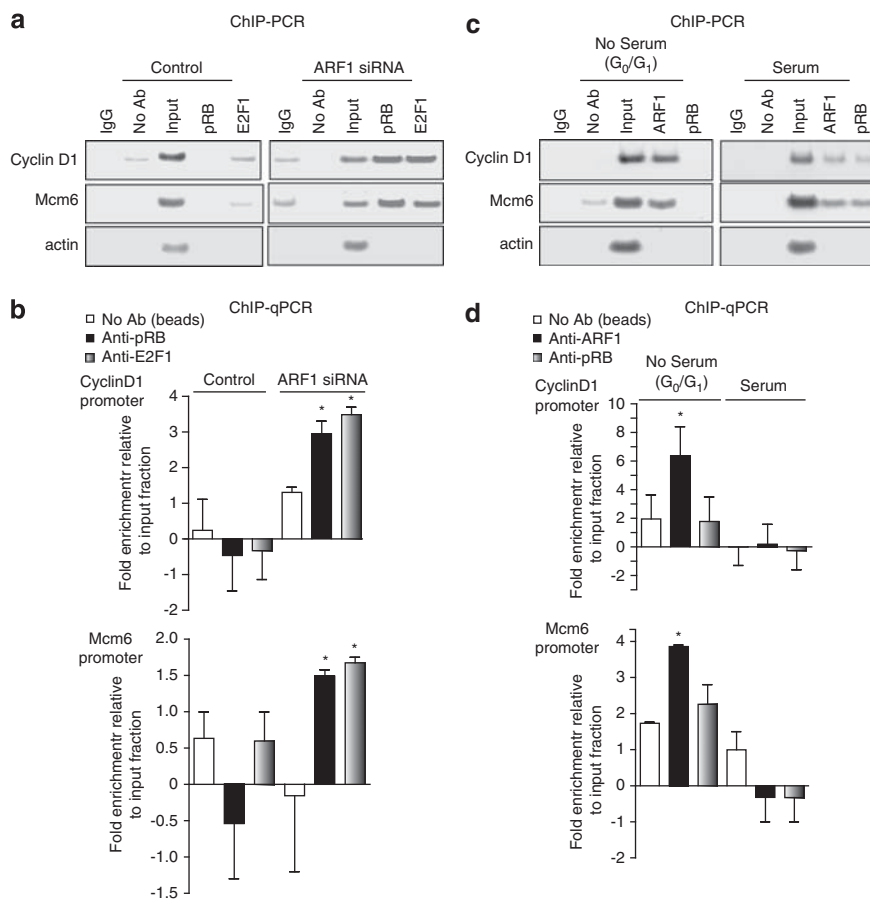


**Figure 6** ARF1 regulates the recruitment of E2F and pRB to E2F-responsive promoters. (a, b) MDA-MB-231 cells were transfected or not with ARF1 siRNA for 7 days and then subjected to ChIP analysis. Interactions of endogenous pRB or E2F1 with cyclin D1 and Mcm6 promoters or  $\beta$ -actin coding region were detected using PCR (a). These results are representative of three independent experiments. Quantifications were performed by qPCR and are expressed as fold enrichment relative to input fraction (b). Quantifications are the mean  $\pm$  s.e.m. of 3 independent experiments. (c, d) MDA-MB-231 cells were serum starved or not for 16 h. Interactions of endogenously expressed ARF1 or pRB with cyclin D1 and Mcm6 promoters or  $\beta$ -actin coding region were assessed by ChIP assays and detected using PCR (c). These results are representative of three independent experiments. Quantifications were performed by qPCR as in (b) and data are expressed as fold enrichment relative to input fraction and are the mean  $\pm$  s.e.m. of three independent experiments (d). \* $P < 0.05$  are values compared with the input.

Interestingly, pRB was also found interacting with cyclin D1 and Mcm6 promoters. To evaluate the enrichment of pRB and E2F1 as a function of the input fraction, we performed quantitative PCR (qPCR) experiments. In control cells, no pRB or E2F1 were enriched at cyclin D1 and Mcm6 promoter sites (Figure 6b). Depletion of ARF1 however led to the recruitment of both pRB and E2F1 at these gene promoter sites. The enrichment of pRB at cyclin D1 and Mcm6 sites was 2.93- and 1.49-fold, respectively, and the enrichment of E2F1 at the same promoter sites was 3.40- and 1.70-fold, respectively. These data suggest that in conditions where ARF1 expression is reduced, the interaction of E2F1 and pRB to their gene promoters is more stable and probably dependent on a less dynamic chromatin.

Finally, we investigated the possibility that ARF1 could interact with cyclin D1 and Mcm6 promoters. ChIP of this GTPase revealed its ability to interact with both gene promoters during G<sub>0</sub>/G<sub>1</sub> phase, but not during proliferative conditions (Figure 6c). qPCR showed that ARF1 enrichment to cyclin D1 and Mcm6 promoter sites was respectively 6.30- and 3.82-fold (Figure 6d). Altogether, these results demonstrate that ARF1 directly impacts pRB/E2F1 interplay, on chromatin, at endogenous sites of E2F1 action.

## Discussion

In invasive breast cancer cells, ARF GTPases are found highly expressed and regulate migration as well as invasion (Hashimoto *et al.*, 2004; Boulay *et al.*, 2008). In this study, we have used two approaches to define the role of ARF1 on cellular proliferation: reduction of expression of this protein by RNA interference, and overexpression of mutants mimicking either an inactive or active form. These strategies allowed us to study the impact of significantly lowering ARF1 levels as well as the consequence of modulating its activation state. Reduction of ARF1 expression in breast cancer cells as well as normal epithelial breast cells limited proliferation. In contrast, expression of an ARF1 mutant mimicking a constitutively activated GTPase enhanced proliferation. Our findings revealed that the molecular mechanism by which ARF1 depletion or inactivation limited proliferation is through the modulation of pRB hyperphosphorylation, its association with E2F1, as well as cell-cycle gene expression, leading to cellular senescence.

We have previously reported that short-term depletion of ARF1 (4 days post transfection) had no effect on basal, but markedly inhibited epidermal growth factor-stimulated proliferation of MDA-MB-231 cells (Boulay *et al.*, 2008). Here, we present evidence that at this time point, inhibition of ARF1 expression already affects the association of pRB with E2F1, although most cells have not yet entered the senescence program. Long-term depletion of ARF1 (4–12 days post transfection) led to impaired basal proliferation rate of both control and

tumor breast epithelial cells. The induction of senescence is considered an effective mechanism to promote permanent cell-cycle arrest, and is mainly associated with pRB and p53 pathways. In MDA-MB-231 cells, p53 is mutated and no longer an effective tumor suppressor (Olivier *et al.*, 2002). In contrast, pRB controls cell-cycle gene expression, thereby limiting cell proliferation. It was previously reported that induction of senescence could take place in non-invasive MCF7 breast cancer cells. For example, retinoic acid treatment first induced a slower cell growth rate between days 4 and 6, a decrease in cell number between day 6 and 9, and finally detectable SA- $\beta$ -gal activity at day 8 (Roninson and Dokmanovic, 2003). Furthermore, senescence was also demonstrated in MDA-MB-231 cells (Sullivan *et al.*, 2008; Bartholomew *et al.*, 2009). In our experiments, SA- $\beta$ -gal activity could be detected as soon as 4 days post transfection to reach a maximum at day 7. Because we were able to revert the induction of senescence promoted by ARF1 depletion when we overexpressed the human papilloma virus E7 oncoprotein, we concluded that the induction of senescence observed was dependent on the RB family of pocket proteins as E7 is known to enhance pRB degradation via the ubiquitin–proteasome pathway (Boyer *et al.*, 1996). We also observed that depletion of ARF1 led to chromatin condensation and appearance of heterochromatin foci, a process detectable by methylation of histone H3 on lysine-9 residue. Condensation of heterochromatic regions is known to silence transcriptional activities of E2F members by inhibiting the availability of gene promoter target sites (Narita *et al.*, 2003). Interestingly, when cells were depleted of ARF1, we observed a significant reduction of cyclin D1, Mcm6 and E2F1 mRNA, as well as protein expression. Altogether, our findings suggest that a strategy aiming at reducing ARF1 levels in breast cancer cells would be effective in limiting tumor growth.

To better define the molecular mechanism by which ARF1 regulated cellular proliferation, we examined pRB in more detail. First, our findings indicated that ARF1 acted specifically on this member of the RB family of proteins. P107 and p130 are also known to bind E2F-responsive promoters, but are rather associated with quiescence (Takahashi *et al.*, 2000; Rayman *et al.*, 2002; Chicas *et al.*, 2010). We found that reduction of ARF1 levels markedly reduced hyperphosphorylation of pRB, suggesting that ARF1 depletion might inhibit cyclin-dependent kinases via a mechanism independent of p16<sup>INK4a</sup> as this cell line exhibits a homologous deletion of this gene (Hui *et al.*, 2000). These findings are further supported by our observation that deletion of ARF1 can also promote senescence of SKBR3 cells, a p16<sup>INK4a</sup>-positive cell line (Hui *et al.*, 2000). In our experiments, depletion of ARF1 led to increased pRB/E2F1 association, suggesting that in conditions where ARF1 cannot become activated, E2F1 is not able to fulfill its main function and act to promote gene transcription to initiate cell-cycle progression. Using ChIP assays, we demonstrated that reduction of ARF1 levels not only markedly contributed to

stabilize the interaction of E2F1 but also pRB, to target gene promoters and repress transcription. We observed that depletion of ARF1 led to a reduction of mRNA and protein levels of cyclin D1, Mcm6 and E2F1, three E2F1 target genes.

To control cell proliferation, we hypothesized that the activation state and the localization of endogenously expressed ARF1 may change during the different phases of the cell cycle. First, when cells were grown in the presence of serum, ARF1 was highly basally activated and mainly present not only at the Golgi but also associated with dynamic plasma membrane ruffles (Boulay *et al.*, 2008). However, when cells were arrested in the G<sub>0</sub>/G<sub>1</sub> phase, amounts of GTP-bound ARF1 markedly decreased and endogenously expressed proteins were found within nuclei, associated with the chromatin at E2F-responsive promoter sites. Levels of cellular activated ARF1 progressively increased during progression through the G<sub>1</sub>/S and M phases of the cell cycle. These results demonstrate that the activation state as well as the cellular localization of ARF1 changes during cell cycle. Although the role of ARF isoforms in carrier vesicle formation is well characterized, it has been speculated by different groups that these proteins may have additional functions. Altan-Bonnet *et al.* (2003) have shown that in mitosis (M phase), ARF1 becomes inactive and is dissociated from the Golgi. These events are essential for chromosome segregation and cytokinesis (Altan-Bonnet *et al.*, 2003). Arl5, an ARF subfamily member, was shown to be present within the chromatin (Lin *et al.*, 2002). In contrast to this Arl isoform, ARF1 does not contain a nuclear localization signal peptide in its sequence or a chromatin-binding domain. Its relocalization to the nucleus might require binding to nucleoporins. ARF guanine-nucleotide exchange factors such as BRAG2 have been detected in nuclei both biochemically and morphologically (Dunphy *et al.*, 2007). Moreover, both BIG1, a guanine-nucleotide exchange factor that is localized to the trans-Golgi network at steady state, and Centaurin  $\alpha$ 1, a GTPase-activating protein for ARF6, have been reported to enter the nucleus and interact with the nucleolar protein nucleolin (Dubois *et al.*, 2003; Padilla *et al.*, 2008). Similarly, PIKE (AGAP2/Centaurin- $\gamma$ 1) was also found within nuclei (Dunphy *et al.*, 2007). In addition, small GTP-binding proteins of the Ran family are best known for their crucial roles in the regulation of nucleocytoplasmic transport and in the function of mitotic spindle (Yudin and Fainzilber, 2009). Similar to other small G proteins, ARF1 may regulate processes in the nucleus, Golgi and at the plasma membrane.

The use of ARF1 mutants has confirmed the importance of this GTPase in the process of cell proliferation. Here, we have shown that expression of ARF1T<sup>31</sup>N, known to sequester ARF guanine-nucleotide exchange factors and prevent activation of endogenously expressed ARF1 proteins, resulted in the inhibition of cell growth, further supporting the hypothesis that ARF1 activation is a key event regulating cell-cycle progression. The observation that overexpression of ARF1Q<sup>71</sup>L, a dominant activating

mutant, enhanced proliferation, further demonstrated the importance of ARF1 activation in this process. Expression of ARF1 mutants was also effective in modulating hyperphosphorylation of pRB. Like depletion of ARF1, expression of the dominant negative form reduced pRB hyperphosphorylation, whereas the dominant activating form further enhanced this effect. In addition, ARF1T<sup>31</sup>N markedly increased the ability of pRB to associate with E2F1 when cells were in the presence of serum, an interaction only observed upon cell-growth arrest. Finally, using ARF1 mutants, we have shown that when this GTPase is inactive, it is able to directly interact with pRB, in chromatin extract. In contrast, a constitutively active form is not present in the chromatin extract and not binding to pRB. The exact role of the ARF1/pRB interaction remains to be defined. Our data clearly demonstrated that the activation state of this GTPase dictates its ability to associate and modulate pRB hyperphosphorylation as well as its association with E2F1, therefore suggesting that a strategy that would impair the ability of this ARF to become activated when highly expressed in invasive breast cancer cells would be effective in limiting dissociation of the pRB/E2F1 complex and cell-cycle progression. The observation that ARF1 depletion and ARF1 inactivation consistently resulted in inhibition of proliferation suggests that it is the activation process of ARF1 that is essential for cell-cycle progression. In G<sub>0</sub>/G<sub>1</sub>, ARF1 becomes mainly under its inactivated form, even though it is highly expressed in MDA-MB-231 cells. However, as cells progress to G<sub>1</sub>/S phase, this GTPase progressively becomes reactivated. Depletion of ARF1 or expression of the dominant negative form would markedly impact this reactivation process of the GTPase. The importance of ARF cycling between a GDP- and GTP-bound form has been demonstrated previously during mitosis (Altan-Bonnet *et al.*, 2003). In light of our findings, ARF1 may have additional roles. Its ability to be recruited to the chromatin upon G<sub>0</sub>/G<sub>1</sub> arrest, directly interact with pRB, and associate with cell-cycle gene promoters suggests that this GTPase may directly control the function of key cell-cycle proteins as well as gene expression. These interesting observations will be important topics for future investigations.

In summary, our findings demonstrate that the GTPase ARF1 is a key regulator of proliferation, a cellular response often misregulated in pathological conditions such as breast cancer. The rapid activation of this molecular switch, following epidermal growth factor stimulation, to control activation of the PI3K/AKT pathway as well as its direct regulation of pRB function makes it an attractive target for novel therapies. In this paper, we show that high levels of active ARF1 (WT or Q<sup>71</sup>L) present in MDA-MB-231 cells contribute to the enhanced proliferative potential of these tumor cells. By being mainly under its GTP-bound form, ARF1 remains outside of the nucleus allowing pRB to be hyperphosphorylated, dissociate from E2F1, and promote cell-cycle gene expression (Figure 7a). Cells growing in serum-deprived media or overexpressing ARF1T<sup>31</sup>N have ARF1 mainly in its

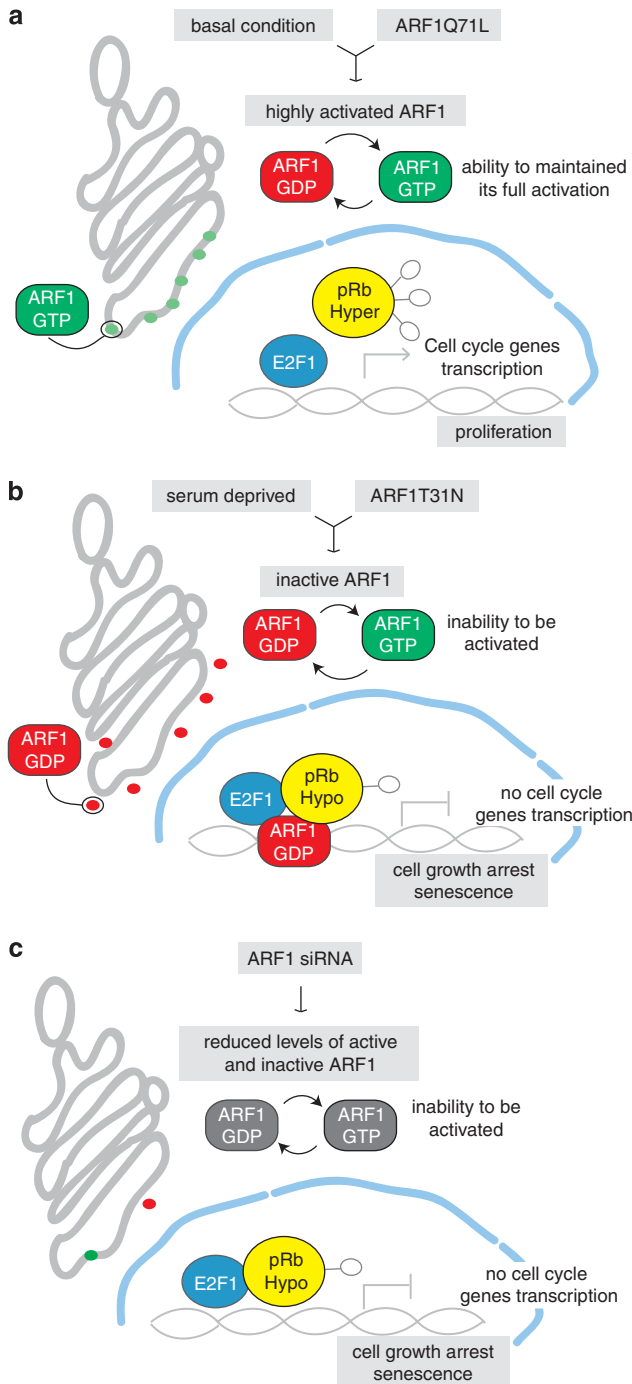


**Figure 7** Model illustrating the role of ARF1 in cell proliferation. (a) In basal condition (media containing serum) or when cells overexpressed ARF1Q71L, ARF1 is highly activated. In these conditions, pRB is hyperphosphorylated, can dissociate from E2F1, which can act to promote cell-cycle gene expression. (b) When cells are deprived of serum or transfected with ARF1T31N, ARF1 is mainly in its inactive form. The GTPase is found in the nucleus, and pRB is mainly hypophosphorylated and in complex with E2F1. Transcription of cell-cycle genes is impaired and proliferation limited. (c) Similarly, depletion of ARF1 impairs the hyperphosphorylation state of pRB and its association to E2F1, prevents cell-cycle gene expression and inhibits cell growth. The sustained inhibition of proliferation in cells expressing ARF1T31N or depletion of ARF1 is due to initiation of replicative senescence.

GDP-bound form. Inactive ARF is free to translocate to the nucleus to associate with pRB. In these conditions, pRB is found mainly hypophosphorylated and associated with E2F1, thereby limiting gene transcription. This results in permanent cell-growth arrest (Figure 7b). Finally, reduction of ARF1 levels leads to a decrease of both active and inactive ARF1. In these conditions, pRB hyperphosphorylation is compromised and as a consequence remains in complex with E2F1, limiting gene transcription. Depletion of ARF1 therefore results in cell-growth arrest (Figure 7c). The cell-growth arrest observed upon transfection of ARF1 siRNA or over-expression of ARF1T31N presented all the biochemical characteristics classically associated with the induction of senescence, such as the formation of SAHF, the constitutive association of pRB and E2F, the stabilization of pRB/E2F1 to E2F-responsive gene promoters, and the decreased expression of cyclin D1 and Mcm6, known to activate Cdk4/6 and be important for pRB hyperphosphorylation and DNA replication (Ewen *et al.*, 1993; Ohtani *et al.*, 1995). Recently, different tools were developed to inhibit ARF activation (Hafner *et al.*, 2006; Viaud *et al.*, 2007). Our results suggest that these or other strategies to limit the ability of ARF1 to become highly activated or expressed could effectively reduce cell proliferation and breast cancer progression.

## Materials and methods

### Reagents and antibodies

Lipofectamine 2000, Alexa-Fluor 488, Alexa-Fluor 568 and Hoescht 33258 were purchased from Invitrogen (Burlington, ON, Canada). Anti-ARF1 (raised against amino acids 174–180: SNQLRNQ of human ARF1 sequence) and anti-H3meK9 antibodies were obtained from Abcam (Cambridge, MA, USA). Anti-pRB, anti-ppRB Ser<sup>795</sup>, anti-E2F1, anti-pan-actin and anti-Histone-3 were from Cell Signaling Technology (Danvers, MA, USA). Anti-p16 (H156), anti-Cdk4, anti-Cyclin D1, anti-p107, anti-p130, anti-GM130 and anti-polyubiquitin (P4D1) were purchased from Santa Cruz Biotech Inc. (Santa Cruz, CA, USA). Mammary epithelium basal medium was from Cambrex Bio Science Walkersville Inc. (Walkersville, MD, USA). All others products were from Sigma Aldrich Company (Oakville, ON, Canada).

### DNA plasmids and siRNAs

siRNA-insensitive ARF1 mutant was previously described (Boulay *et al.*, 2008). Double-stranded scrambled ARF1 siRNA with 19-nucleotide duplex RNA and 2-nucleotide 3' dTdT overhangs were previously described (Houndolo *et al.*, 2005; Cotton *et al.*, 2007). All siRNAs were synthesized using the Silencer siRNA Construction Kit from Ambion (Austin, TX, USA). p16<sup>INK4a</sup> cDNAs in lentivirus were obtained from Dr Christian Beauséjour (University of Montreal, QC, Canada).

### Cell culture, transfection and infection

MDA-MB-231, SKBR3 and COS-7 cells were maintained in Dulbecco's modified Eagle's medium supplemented with 10% fetal bovine serum (FBS). BT474 and T47D cells were maintained in Dulbecco's modified Eagle's medium:Ham's F12 supplemented with 10% FBS, whereas MCF10A cells

were maintained in mammary epithelium basal medium supplemented with 0.52 mg/ml bovine pituitary extract, 10 ng/ml recombinant epidermal growth factor, 10 µg/ml insulin, 1 µg/ml hydrocortisone, 0.1 mg/ml gentamycin and 0.1 µg/ml amphotericin B. All cells were maintained at 37 °C and 5% CO<sub>2</sub>. Cells were transfected with DNA and/or siRNA using Lipofectamine 2000, according to the manufacturer's instructions. Cells were infected with p16<sup>INK4a</sup> cDNA expressed in p-lenti plasmids using lentivirus as described (Beausejour *et al.*, 2003).

#### Growth assay

Cells were transiently transfected, trypsinized and equal numbers (1 × 10<sup>4</sup> cells) were reseeded in a 10-cm dish for all transfection conditions. After 24 h, the media was changed for fresh complete media (10% FBS) and all sets of cells were left for 12 days. For each indicated time point, cells were trypsinized and counted.

#### Soft-agar growth assay

MDA-MB-231 cells were transiently transfected with siRNA (scrambled or ARF1, 25 nM) or with plasmid DNA (pBKΔ or ARF1T<sup>31N</sup>). Soft-agar assays were performed by seeding 2 × 10<sup>3</sup> transfected cells in Dulbecco's modified Eagle's medium containing 0.2% agarose in a 10-cm dish, coated with a layer of 0.8% agarose/Dulbecco's modified Eagle's medium.

#### Senescence associated with β-gal assay

Cells were transiently transfected with siRNA (scrambled or ARF1, 25 nM for 72 h) or plasmid DNA (pBKΔ, ARF1 or ARF1T<sup>31N</sup>). Cells were washed twice in phosphate-buffered saline (PBS) and fixed with 10% formalin solution for 5 min at room temperature. Cells were washed again twice and then incubated for 16 h in staining solution (40 mM; citric acid/phosphate buffer pH 6.0, 5 mM; potassium ferricyanide, 5 mM; potassium ferrocyanide, 150 mM; sodium chloride, 2 mM; dichloride magnesium and 1 mg/ml; 5-bromo-4-chloro-3-indolyl-β-D-galactopyranoside) in a 37 °C chamber. Pictures were taken using a × 40 magnification with a Zeiss Axioskop microscope (Carl Zeiss Microscopy, Jena, Germany) connected to a SPOT Digital Camera (Diagnostic Instruments Inc., Sterling Heights, MI, USA).

#### Western blotting

Whole-cell lysates were harvested in 100 µl of Triton/glycerol/4-(2-hydroxyethyl)-1-piperazineethanesulfonic acid buffer (pH 7.3, 1% Triton X-100, 10% glycerol, 50 mM NaCl, 50 mM 4-(2-hydroxyethyl)-1-piperazineethanesulfonic acid, 5 mM EDTA) complemented with protease inhibitors and 1 mM sodium orthovanadate. Whole-cell lysates were solubilized (4 °C, 1 h), and total soluble proteins (40 µg) were loaded onto polyacrylamide gels and transferred onto nitrocellulose membranes. The membranes were blotted for relevant proteins using specific primary antibodies (described for each experiment). Secondary antibodies were all fluorescein isothiocyanate-conjugated and fluorescence was detected using a Typhoon 9410 scanner (GE Healthcare Life Sciences, Baie d'Urfe, QC, Canada). Quantification of the digital images obtained was performed using ImageQuant 5.2 software.

#### Cell fractionation

Cells were harvested in 100 µl of PBS containing protease inhibitors and passed three times through a 27G 1/2 syringe. Samples were spun at 500 g for 10 min, at 4 °C. Supernatants were spun at 100 000 r.p.m. for 30 min, at 4 °C, to separate

membrane (pellet) and cytosol (supernatant). Whole nuclear extracts were obtained by solubilizing the pellets from the 500 g centrifugation in Buffer I (160 mM sodium chloride, 38 mM 4-(2-hydroxyethyl)-1-piperazineethanesulfonic acid pH: 7.4, 1 mM dichloride magnesium and 1 mM ethylene glycol tetraacetic acid) containing protease inhibitors. Samples were put on ice for 30 min and then spun at 14 000 r.p.m. for 30 min. For chromatin fractions, cells were harvested in 100 µl of buffer I containing protease inhibitors and put on ice for 5 min. Nuclei were isolated by centrifugation at 500 g for 10 min, at 4 °C. Pellets were resuspended in buffer II (100 mM 1,4-piperazinediethane sulfonic acid pH:6.8, 300 mM sodium chloride, 300 mM sucrose, 3 mM dichloride magnesium, 1 mM ethylene glycol tetraacetic acid, 1 mM dithiothreitol and 0.5% Triton X-100) containing protease inhibitors. Insoluble chromatin fraction were collected by centrifugation (600 g for 5 min, at 4 °C) and then washed once in buffer II containing protease inhibitors. Samples were run on a 10 or 14% polyacrylamide gel. Proteins were detected by immunoblot analysis using specific antibodies.

#### Real-time PCR

For real-time reverse transcription-PCR, 5 µg of total mRNA was reverse-transcribed using the High Capacity cDNA Reverse Transcription Kit with random primers (Applied Biosystems, CA, USA). As previously described (Boulay *et al.*, 2008), gene expression levels were determined using primers and probe sets from Applied Biosystems (ABI Gene Expression Assays). Primers for pRB, E2F1, Cyclin D1 and Mcm6 are available upon request.

#### ARF1 activation

Cells were plated in 6-well dishes and may or treated or not with fresh serum medium or with hydroxyurea (20 µM) or vincristine (1 µM) at 37 °C for 16 h, and activation of ARF1 was performed as described (Cotton *et al.*, 2007). Briefly, cells were lysed in 60 µl of ice-cold lysis buffer E (pH 7.4, 50 mM Tris-HCl, 1% Nonidet P-40, 137 mM NaCl, 10% glycerol, 5 mM MgCl<sub>2</sub>, 20 mM NaF, 1 mM NaPPi, 1 mM Na<sub>3</sub>VO<sub>4</sub> and protease inhibitors). Samples were incubated for 30 min (4 °C) and spun for 10 min at 10 000 r.p.m. Glutathione S-transferase-golgo-associated, gamma adaptin ear containing, ARF binding protein 3 coupled to glutathione sepharose 4B were added to each tube and samples were rotated at 4 °C for 1 h. Proteins were eluted in 25 µl SDS sample buffer by heating to 65 °C for 15 min. Detection of ARF1-GTP was performed by immunoblot analysis using a specific anti-ARF1 antibody.

#### Microscopy

Cells were serum starved or not for 16 h, fixed using paraformaldehyde (4%) for 15 min at room temperature. For detection of endogenous ARF1, cells were stained with a monoclonal anti-ARF1 antibody and then with an anti-mouse antibody coupled to Alexa-Fluor 488. For some conditions, cells were subsequently incubated with Hoescht 33258 for 10 min. Images were acquired using a × 63 oil immersion objective (Carl Zeiss Inc., Oberkochen, Germany) on a Zeiss LSM-510 META laser scanning microscope (Carl Zeiss Inc.). To determine SAHF-positive cells, these were stained with a polyclonal anti-H3meK9 antibody and then with an anti-rabbit antibody coupled to Alexa-Fluor 568. Cells were then fixed, mounted onto slides using Gel Tol mounting medium. Pictures were taken using a × 40 magnification with a Zeiss Axioskop microscope (Carl Zeiss Microscopy) connected to a SPOT Digital Camera (Diagnostic Instruments Inc., Sterling Heights, MI, USA).

### Co-immunoprecipitation experiments

MDA-MB-231 cells were treated or not with fresh medium for 16 h. Co-immunoprecipitation experiments were described previously (Boulay *et al.*, 2008). When Co-immunoprecipitation was performed in whole-cell lysates or chromatin fractions, cells were lysed into Triton/glycerol/4-(2-hydroxyethyl)-1-piperazineethanesulfonic acid buffer (100  $\mu$ l) or lysed using the cell fractionation protocol, respectively. Interacting ARF1, pRB or E2F1 was assessed by western blot analysis.

### GST-pulldown assay

Equal amounts of GST and GST-pRB were incubated in buffer NETN (20 mM Tris pH 8.0, 1 mM EDTA pH 8.0, 0.5% Nonidet, 1 mM dithiothreitol, 0.5 mg/ml bovine serum albumin (BSA), 100 mM sodium chloride and protease inhibitors) with 1  $\mu$ g of purified recombinant ARF1 protein. ARF1 loading was performed using GDP $\beta$ S (100  $\mu$ M) or GTP $\gamma$ S (10  $\mu$ M) in buffer NETN in a final volume of 250  $\mu$ l. Loading of nucleotide was arrested with MgCl<sub>2</sub> (60 mM) after 30 min at 30 °C, and then samples were mixed with GST-pRB for a final volume of 250  $\mu$ l. In some experiments, GST and GST-pRB were incubated with IgG or Cdk4 immunoprecipitated from MDA-MB-231 cells, as described above using a specific anti-Cdk4 antibody, in a kinase buffer (Tris 20 mM pH 7.5, MgCl<sub>2</sub> 7.5 mM, dithiothreitol 1 mM, ethylene glycol tetraacetic acid 0.5 mM) for 1 h at 30 °C. Kinase reaction was stopped by adding 10  $\mu$ l of GST glutathione sepharose 4B beads, and then put on ice for 20 min. Samples were rotated for 4 h at 4 °C. Beads were recovered by centrifugation, washed five times, and proteins were eluted into 20  $\mu$ l of SDS sample buffer by heating to 65 °C for 15 min. All samples were run on a 10 or 14% polyacrylamide gel, and pRB/ARF1 interaction was detected by western blotting using a specific anti-ARF1 antibody and an anti-pRB antibody. GST-pRB was a gift from Dr Tony Kouzarides (The Gurdon Institute and Department of Pathology, University of Cambridge, Cambridge, UK).

### ChIP assay

Methods were modified from Takahashi *et al.* (2000). Briefly, a first set of MDA-MB-231 cells was transfected or not with ARF1 siRNA (25 nM) for 7 days. A second set of cells was incubated in the absence or presence of fresh medium (16 h). All cells were treated with 1.5% formaldehyde for 10 min at room temperature, and then incubated with glycine (125 mM) for 5 min. Cells were washed twice with PBS, harvested in cold PBS containing protease inhibitors, spun at 700 g for 5 min, and washed once with PBS. Pellets were successively resuspended in ChIP1 buffer (EDTA 2 mM, SDS 0.1%, Tris-HCl 20 mM pH 7.5, Triton X-100 1%, containing protease inhibitors), and ChIP2 buffer (EDTA 1 mM, SDS 0.1%, Tris-HCl 20 mM pH 8.0, Triton X-100%, NaCl 150 mM, containing protease inhibitors). Samples were sonicated to generate DNA fragments of approximately 500 bp. For immunoprecipitation experiments, 0.5 mg of protein extract was precleared for 3 h with 25  $\mu$ l of a 50% slurry of protein A/G agarose beads and 6  $\mu$ g of salmon sperm DNA at 4 °C. Anti-pRB, anti-E2F1, anti-ARF1 antibodies or beads alone (no Ab) were incubated with the samples overnight at 4 °C. Immunoprecipitates were recovered by a 2 h-incubation at 4 °C with 25  $\mu$ l of a 50% slurry of protein A/G agarose beads. Precipitates were washed three times with ChIP3 buffer (EDTA 1 mM, SDS 0.1%, Tris-HCl 20 mM pH 8.0, Triton X-100%, NaCl 150 mM, 500 mM LiCl). Immunocomplexes were eluted for 10 min at 65 °C with 1% SDS and crosslinking was reversed by adding an equal volume of TE, NaCl (up to 200 mM) and RNase (10 mg), by

incubating overnight at 65 °C. After 2 h of proteinase K treatment, DNA was extracted with phenol/chloroform and chloroform. Samples were then precipitated with 0.2 M NaCl (containing 20 mg of glycogen carrier) and 2.5 volumes of ethyl alcohol before being resuspended in 60  $\mu$ l of TE buffer. First, PCR reactions were performed using 2  $\mu$ l of each sample. Forward and reverse primers (250 nM), dNTP (0.2 mM), plaque forming unit (PFU) MgSO<sub>4</sub> buffer (1  $\times$ ), and PFU (0.5 unit) were added to a final volume of 20  $\mu$ l. PCR were performed using a thermocycler T-Personnal Biometra (Montreal Biotech, Kirkland, ON, Canada) to amplify E2F-responsive promoter regions. Second, qPCR reactions were performed using universal probe library for actin or SYBR green assays for Mcm6 and Cyclin D1. Gene expression level was determined using assays designed with the universal probe library (<http://www.universalprobelibrary.com>) from Roche, Laval, QC, Canada. qPCR reactions were performed using 1.5  $\mu$ l of cDNA samples (5–25 ng), 5  $\mu$ l of the TaqMan Fast Universal PCR Master Mix (Applied Biosystems), 2  $\mu$ M of each primer, and 1  $\mu$ M of a universal probe library probe #17 in a total volume of 10  $\mu$ l. SYBR green qPCR reactions were performed using 1.5  $\mu$ l of cDNA samples (5–25 ng), 5  $\mu$ l of the Fast SYBR Green Master Mix (Applied Biosystems), and 2  $\mu$ M of each primer in a total volume of 10  $\mu$ l. Melting curves were performed using dissociation curve software (sequence detection system (SDS) 2.2.2; Applied Biosystems) to ensure only a single product was amplified. The ABI PRISM 7900HT Sequence Detection System (Applied Biosystems) was used to detect the amplification level and was programmed with an initial step of 3 min at 95 °C, followed by 40 cycles of the following: 5 s at 95 °C and 30 s at 60 °C. All reactions were run in triplicate and the average values of threshold cycles (Ct) were used for quantification. The relative quantification of target genes was determined using the  $\Delta\Delta$ CT method. Briefly, the Ct values of target genes were normalized to an endogenous actin control gene ( $\Delta$ CT = Ct<sub>target</sub> – Ct<sub>CTL</sub>) and compared with a calibrator:  $\Delta\Delta$ CT =  $\Delta$ Ct<sub>sample</sub> –  $\Delta$ Ct<sub>calibrator</sub>. Relative expression (RQ) was calculated using the SDS 2.2.2 software and the formula is  $RQ = 2^{-\Delta\Delta CT}$ . Primer sequences are available upon request.

### Statistical analysis

Statistical analysis was performed using a one-way and two-way analysis of variance followed by a Bonferroni's multiple comparison tests using GraphPad Prism (ver. 4.0a; San Diego, CA, USA).

### Conflict of interest

The authors declare no conflict of interest.

### Acknowledgements

We would like to thank Dr Tony Kouzarides (The Gurdon Institute, University of Cambridge, UK) for GST-pRB. We thank Raphaëlle Lambert from genomic platform of IRIC (Montreal, Canada). We are grateful to Dr Christian Beauséjour (University of Montreal, Montreal, Canada) for reagents and helpful discussion. We thank Dr Stéphane A Laporte (McGill University, Montreal, Canada) for the use of his confocal microscope and Dr Denis de Blois and Julie-Émilie Huot-Marchand (University of Montreal, Montreal, Canada) for the use of their photo-microscopy platform. We thank Dr Véronique Bourdeau (University

of Montreal, Montreal, Canada) for helpful discussion and critical reading of the paper. This work was supported by the Canadian Institutes of Health Research (CIHR) grant

MOP-79470 to AC. PLB is the recipient of a Frederick Banting and Charles Best PhD Research Award from the CIHR. AC is the recipient of a New Investigator Award from the CIHR.

## References

- Altan-Bonnet N, Phair RD, Polishchuk RS, Weigert R, Lippincott-Schwartz J. (2003). A role for Arf1 in mitotic Golgi disassembly, chromosome segregation, and cytokinesis. *Proc Natl Acad Sci USA* **100**: 13314–13319.
- Azab AK, Azab F, Blotta S, Pitsillides CM, Thompson B, Runnels JM *et al.* (2009). RhoA and Rac1 GTPases play major and differential roles in stromal cell-derived factor-1-induced cell adhesion and chemotaxis in multiple myeloma. *Blood* **114**: 619–629.
- Bartholomew JN, Volonte D, Galbiati F. (2009). Caveolin-1 regulates the antagonistic pleiotropic properties of cellular senescence through a novel Mdm2/p53-mediated pathway. *Cancer Res* **69**: 2878–2886.
- Beausejour CM, Krtolica A, Galimi F, Narita M, Lowe SW, Yaswen P *et al.* (2003). Reversal of human cellular senescence: roles of the p53 and p16 pathways. *Embo J* **22**: 4212–4222.
- Boulay PL, Cotton M, Melancon P, Claing A. (2008). ADP-ribosylation factor 1 controls the activation of the phosphatidylinositol 3-kinase pathway to regulate epidermal growth factor-dependent growth and migration of breast cancer cells. *J Biol Chem* **283**: 36425–36434.
- Boyer SN, Wazer DE, Band V. (1996). E7 protein of human papilloma virus-16 induces degradation of retinoblastoma protein through the ubiquitin-proteasome pathway. *Cancer Res* **56**: 4620–4624.
- Burkhardt DL, Sage J. (2008). Cellular mechanisms of tumour suppression by the retinoblastoma gene. *Nat Rev Cancer* **8**: 671–682.
- Chellappan S, Kraus VB, Kroger B, Munger K, Howley PM, Phelps WC *et al.* (1992). Adenovirus E1A, simian virus 40 tumor antigen, and human papillomavirus E7 protein share the capacity to disrupt the interaction between transcription factor E2F and the retinoblastoma gene product. *Proc Natl Acad Sci USA* **89**: 4549–4553.
- Chicas A, Wang X, Zhang C, McCurrach M, Zhao Z, Mert O *et al.* (2010). Dissecting the unique role of the retinoblastoma tumor suppressor during cellular senescence. *Cancer Cell* **17**: 376–387.
- Cohen LA, Honda A, Varnai P, Brown FD, Balla T, Donaldson JG. (2007). Active Arf6 recruits ARNO/cytohesin GEFs to the PM by binding their PH domains. *Mol Biol Cell* **18**: 2244–2253.
- Cotton M, Boulay PL, Houndolo T, Vitale N, Pitcher JA, Claing A. (2007). Endogenous ARF6 interacts with Rac1 upon angiotensin II stimulation to regulate membrane ruffling and cell migration. *Mol Biol Cell* **18**: 501–511.
- Courtois-Cox S, Jones SL, Cichowski K. (2008). Many roads lead to oncogene-induced senescence. *Oncogene* **27**: 2801–2809.
- D'Souza-Schorey C, Chavrier P. (2006). ARF proteins: roles in membrane traffic and beyond. *Nat Rev Mol Cell Biol* **7**: 347–358.
- Der CJ, Krontiris TG, Cooper GM. (1982). Transforming genes of human bladder and lung carcinoma cell lines are homologous to the ras genes of Harvey and Kirsten sarcoma viruses. *Proc Natl Acad Sci USA* **79**: 3637–3640.
- Dimri GP, Campisi J. (1994). Molecular and cell biology of replicative senescence. *Cold Spring Harb Symp Quant Biol* **59**: 67–73.
- Dubois T, Zemlickova E, Howell S, Aitken A. (2003). Centaurin-alpha 1 associates *in vitro* and *in vivo* with nucleolin. *Biochem Biophys Res Commun* **301**: 502–508.
- Dunphy JL, Ye K, Casanova JE. (2007). Nuclear functions of the Arf guanine nucleotide exchange factor BRAG2. *Traffic* **8**: 661–672.
- Duro D, Bernard O, Della Valle V, Berger R, Larsen CJ. (1995). A new type of p16INK4/MTS1 gene transcript expressed in B-cell malignancies. *Oncogene* **11**: 21–29.
- Ewen ME, Sluss HK, Sherr CJ, Matsushima H, Kato J, Livingston DM. (1993). Functional interactions of the retinoblastoma protein with mammalian D-type cyclins. *Cell* **73**: 487–497.
- Ferbeyre G, de Stanchina E, Lin AW, Querido E, McCurrach ME, Hannon GJ *et al.* (2002). Oncogenic ras and p53 cooperate to induce cellular senescence. *Mol Cell Biol* **22**: 3497–3508.
- Galas MC, Helms JB, Vitale N, Thierse D, Aunis D, Bader MF. (1997). Regulated exocytosis in chromaffin cells. A potential role for a secretory granule-associated ARF6 protein. *J Biol Chem* **272**: 2788–2793.
- Gluzman Y. (1981). SV40-transformed simian cells support the replication of early SV40 mutants. *Cell* **23**: 175–182.
- Hafner M, Schmitz A, Grune I, Srivatsan SG, Paul B, Kolanus W *et al.* (2006). Inhibition of cytohesins by SecinH3 leads to hepatic insulin resistance. *Nature* **444**: 941–944.
- Hashimoto S, Onodera Y, Hashimoto A, Tanaka M, Hamaguchi M, Yamada A *et al.* (2004). Requirement for Arf6 in breast cancer invasive activities. *Proc Natl Acad Sci USA* **101**: 6647–6652.
- Houndolo T, Boulay PL, Claing A. (2005). G protein-coupled receptor endocytosis in ARF6-depleted cells. *J Biol Chem* **280**: 5598–5604.
- Hui R, Macmillan RD, Kenny FS, Musgrove EA, Blamey RW, Nicholson RI *et al.* (2000). INK4a gene expression and methylation in primary breast cancer: overexpression of p16INK4a messenger RNA is a marker of poor prognosis. *Clin Cancer Res* **6**: 2777–2787.
- Larrea MD, Hong F, Wander SA, da Silva TG, Helfman D, Lannigan D *et al.* (2009). RSK1 drives p27Kip1 phosphorylation at T198 to promote RhoA inhibition and increase cell motility. *Proc Natl Acad Sci USA* **106**: 9268–9273.
- Liang J, Zubovitz J, Petrocelli T, Kotchetkov R, Connor MK, Han K *et al.* (2002). PKB/Akt phosphorylates p27, impairs nuclear import of p27 and opposes p27-mediated G1 arrest. *Nat Med* **8**: 1153–1160.
- Lin CY, Li CC, Huang PH, Lee FJ. (2002). A developmentally regulated ARF-like 5 protein (ARL5), localized to nuclei and nucleoli, interacts with heterochromatin protein 1. *J Cell Sci* **115**: 4433–4445.
- Mallette FA, Ferbeyre G. (2007). The DNA damage signaling pathway connects oncogenic stress to cellular senescence. *Cell Cycle* **6**: 1831–1836.
- Manning BD, Cantley LC. (2007). AKT/PKB signaling: navigating downstream. *Cell* **129**: 1261–1274.
- Miller CL, Arnold MM, Broering TJ, Eichwald C, Kim J, Dinoso JB *et al.* (2007). Virus-derived platforms for visualizing protein associations inside cells. *Mol Cell Proteomics* **6**: 1027–1038.
- Mitchell R, Robertson DN, Holland PJ, Collins D, Lutz EM, Johnson MS. (2003). ADP-ribosylation factor-dependent phospholipase D activation by the M3 muscarinic receptor. *J Biol Chem* **278**: 33818–33830.
- Motti ML, Califano D, Troncone G, De Marco C, Migliaccio I, Palmieri E *et al.* (2005). Complex regulation of the cyclin-dependent kinase inhibitor p27kip1 in thyroid cancer cells by the PI3K/AKT pathway: regulation of p27kip1 expression and localization. *Am J Pathol* **166**: 737–749.
- Mythreye K, Blobe GC. (2009). The type III TGF-beta receptor regulates epithelial and cancer cell migration through beta-arrestin2-mediated activation of Cdc42. *Proc Natl Acad Sci USA* **106**: 8221–8226.
- Narita M, Nunez S, Heard E, Narita M, Lin AW, Hearn SA *et al.* (2003). Rb-mediated heterochromatin formation and silencing of E2F target genes during cellular senescence. *Cell* **113**: 703–716.
- Narita Y, Nagane M, Mishima K, Huang HJ, Furnari FB, Cavenee WK. (2002). Mutant epidermal growth factor receptor signaling down-regulates p27 through activation of the phosphatidylinositol 3-kinase/Akt pathway in glioblastomas. *Cancer Res* **62**: 6764–6769.
- Nevins JR, Chellappan SP, Mudryj M, Hiebert S, Devoto S, Horowitz J *et al.* (1991). E2F transcription factor is a target for the RB protein and the cyclin A protein. *Cold Spring Harb Symp Quant Biol* **56**: 157–162.
- Ohtani K, DeGregori J, Nevins JR. (1995). Regulation of the cyclin E gene by transcription factor E2F1. *Proc Natl Acad Sci USA* **92**: 12146–12150.

- Ohtani K, Iwanaga R, Nakamura M, Ikeda M, Yabuta N, Tsuruga H *et al.* (1999). Cell growth-regulated expression of mammalian MCM5 and MCM6 genes mediated by the transcription factor E2F. *Oncogene* **18**: 2299–2309.
- Olivier M, Eeles R, Hollstein M, Khan MA, Harris CC, Hainaut P. (2002). The IARC TP53 database: new online mutation analysis and recommendations to users. *Hum Mutat* **19**: 607–614.
- Padilla PI, Uhart M, Pacheco-Rodriguez G, Peculis BA, Moss J, Vaughan M. (2008). Association of guanine nucleotide-exchange protein BIG1 in HepG2 cell nuclei with nucleolin, U3 snoRNA, and fibrillarin. *Proc Natl Acad Sci USA* **105**: 3357–3361.
- Parada LF, Tabin CJ, Shih C, Weinberg RA. (1982). Human EJ bladder carcinoma oncogene is homologue of Harvey sarcoma virus ras gene. *Nature* **297**: 474–478.
- Rayman JB, Takahashi Y, Indjeian VB, Dannenberg JH, Catchpole S, Watson RJ *et al.* (2002). E2F mediates cell cycle-dependent transcriptional repression *in vivo* by recruitment of an HDAC1/mSin3B corepressor complex. *Genes Dev* **16**: 933–947.
- Roninson IB, Dokmanovic M. (2003). Induction of senescence-associated growth inhibitors in the tumor-suppressive function of retinoids. *J Cell Biochem* **88**: 83–94.
- Serrano M, Lin AW, McCurrach ME, Beach D, Lowe SW. (1997). Oncogenic ras provokes premature cell senescence associated with accumulation of p53 and p16INK4a. *Cell* **88**: 593–602.
- Soule HD, Maloney TM, Wolman SR, Peterson Jr WD, Brenz R, McGrath CM *et al.* (1990). Isolation and characterization of a spontaneously immortalized human breast epithelial cell line, MCF-10. *Cancer Res* **50**: 6075–6086.
- Stearns T, Willingham MC, Botstein D, Kahn RA. (1990). ADP-ribosylation factor is functionally and physically associated with the Golgi complex. *Proc Natl Acad Sci USA* **87**: 1238–1242.
- Sullivan R, Pare GC, Frederiksen LJ, Semenza GL, Graham CH. (2008). Hypoxia-induced resistance to anticancer drugs is associated with decreased senescence and requires hypoxia-inducible factor-1 activity. *Mol Cancer Ther* **7**: 1961–1973.
- Sun P, Yoshizuka N, New L, Moser BA, Li Y, Liao R *et al.* (2007). PRAK is essential for ras-induced senescence and tumor suppression. *Cell* **128**: 295–308.
- Takahashi Y, Rayman JB, Dynlacht BD. (2000). Analysis of promoter binding by the E2F and pRB families *in vivo*: distinct E2F proteins mediate activation and repression. *Genes Dev* **14**: 804–816.
- Takano Y, Takenaka H, Kato Y, Masuda M, Mikami T, Saegusa M *et al.* (1999). Cyclin D1 overexpression in invasive breast cancers: correlation with cyclin-dependent kinase 4 and oestrogen receptor overexpression, and lack of correlation with mitotic activity. *J Cancer Res Clin Oncol* **125**: 505–512.
- Tonic I, Yu WN, Park Y, Chen CC, Hay N. (2010). Akt activation emulates Chk1 inhibition and Bcl2 overexpression and abrogates G2 cell cycle checkpoint by inhibiting BRCA1 foci. *J Biol Chem* **285**: 23790–23798.
- Vernier M, Bourdeau V, Gaumont-Leclerc MF, Moiseeva O, Begin V, Saad F *et al.* (2011). Regulation of E2Fs and senescence by PML nuclear bodies. *Genes Dev* **25**: 41–50.
- Viaud J, Zeghouf M, Barelli H, Zeeh JC, Padilla A, Guibert B *et al.* (2007). Structure-based discovery of an inhibitor of Arf activation by Sec7 domains through targeting of protein-protein complexes. *Proc Natl Acad Sci USA* **104**: 10370–10375.
- Watanabe G, Albanese C, Lee RJ, Reutens A, Vairo G, Henglein B *et al.* (1998). Inhibition of cyclin D1 kinase activity is associated with E2F-mediated inhibition of cyclin D1 promoter activity through E2F and Sp1. *Mol Cell Biol* **18**: 3212–3222.
- Weinberg RA. (1995). The retinoblastoma protein and cell cycle control. *Cell* **81**: 323–330.
- Wu D, Asiedu M, Wei Q. (2009). Myosin-interacting guanine exchange factor (MyoGEF) regulates the invasion activity of MDA-MB-231 breast cancer cells through activation of RhoA and RhoC. *Oncogene* **28**: 2219–2230.
- Yagata H, Kajiura Y, Yamauchi H. (2011). Current strategy for triple-negative breast cancer: appropriate combination of surgery, radiation, and chemotherapy. *Breast Cancer* (e-pub ahead of print).
- Yakes FM, Chinratanalab W, Ritter CA, King W, Seelig S, Arteaga CL. (2002). Herceptin-induced inhibition of phosphatidylinositol-3 kinase and Akt is required for antibody-mediated effects on p27, cyclin D1, and antitumor action. *Cancer Res* **62**: 4132–4141.
- Yudin D, Fainzilber M. (2009). Ran on tracks—cytoplasmic roles for a nuclear regulator. *J Cell Sci* **122**: 587–593.
- Zhou BP, Liao Y, Xia W, Zou Y, Spohn B, Hung MC. (2001). HER-2/neu induces p53 ubiquitination via Akt-mediated MDM2 phosphorylation. *Nat Cell Biol* **3**: 973–982.

Supplementary Information accompanies the paper on the Oncogene website (<http://www.nature.com/onc>)